Available online at www.sciencedirect.com
SCIENCE DIRECT®
Journal of Sound and Vibration 272 (2004) 495–511
JOURNAL OF SOUND AND VIBRATION
www.elsevier.com/locate/jsvi

Fault tolerance of homopolar magnetic bearings

Uhn Joo Na*

Rotordynamics Group, Structural Systems Department, Korea Institute of Machinery & Materials, 171 Jang-dong, Yusung-gu, Taejon 305-343, South Korea

Received 9 December 2002; accepted 26 March 2003

Abstract

This paper develops the theory for a fault-tolerant, permanent magnet biased, homopolar magnetic bearing. If some of the coils or power amplifiers suddenly fail, the remaining coil currents change via a novel distribution matrix such that the same magnetic forces are maintained before and after failure. Lagrange multiplier optimization with equality constraints is utilized to calculate the optimal distribution matrix that maximizes the load capacity of the failed bearing. Some numerical examples of distribution matrices are provided to illustrate the new theory. Simulations show that very much the same dynamic responses (orbits or displacements) are maintained throughout failure events (up to any combination of 5 coils failed for the 8 pole magnetic bearing) while currents and fluxes change significantly. The overall load capacity of the bearing actuator is reduced as coils fail. The same magnetic forces are then preserved up to the load capacity of the failed bearing.

1. Introduction

A magnetic bearing system is a mechatronics device consisting of a magnetic force actuator (an active magnetic bearing, or AMB), motion sensors, power amplifiers, and a feedback controller (DSP), that suspends the spinning rotor magnetically without physical contact, and suppresses vibrations. Magnetic bearings find greater use in high speed, high performance applications since they have many advantages over conventional fluid film or rolling element bearings, such as lower friction losses, lubrication free, temperature extremes, no wear, quiet, high speed operations, actively adjustable stiffness and damping, and dynamic force isolation. Though magnetic bearings find more applications in industry, reliability requirements limit magnetic bearings from being

*Tel.: +82-2-868-7666.
E-mail address: ujna@kimm.re.kr (U.J. Na).

0022-460X/03/$ - see front matter © 2003 Elsevier Ltd. All rights reserved.
doi:10.1016/S0022-460X(03)00379-1

used in highly critical applications. Failure of components such as coils or power amplifiers in magnetic bearings may result in a failure of the entire system.

Fault tolerant control provides continued operation of magnetic bearing actuators even if its power amplifiers or coils suddenly fail. Much research has been devoted to fault-tolerant heteropolar magnetic bearings. Maslen and Meeker [1] introduced a fault-tolerant 8-pole heteropolar magnetic bearing actuator with independently controlled currents and experimentally verified it in Maslen et al. [2]. Flux coupling in a heteropolar magnetic bearing allows the remaining coils to produce force resultants identical to the unfailed bearing, if the remaining coil currents are properly redistributed. Na and Palazzolo [3,4] also investigated the optimized realization of fault-tolerant magnetic bearing actuators and experimentally showed it on a flexible rotor such that rotor displacements after failure can be maintained close to the displacements before failure for up to all combinations of 4 coils failed and certain combinations of 5 coils failed out of 8 coils. Na and Palazzolo [5] introduced a fault-tolerant control scheme utilizing the grouping of currents to reduce the required number of controller outputs and to remove decoupling chokes.

To the best of the authors' knowledge no fault-tolerant control algorithm has been developed for the permanent magnet biased homopolar magnetic bearings. Homopolar magnetic bearings have a unique biasing scheme that directs the bias flux flow into the active pole plane where it energizes the working air gaps, and then returns through the other pole plane (either active or dead) and the shaft sleeve. Homopolar magnetic bearings yield a very high efficiency when the permanent magnets are used as the source of bias flux to energize the air gaps and the electromagnetic coils are used to supply control fluxes. Unique flux paths of mixed axial/radial orientation in homopolar design help to lower eddy current power losses significantly [6]. Some of the results on modelling, design, and control of homopolar magnetic bearings are shown in literature. Sortore et al. [7] and Allaire et al. [8] presented design methods and experimental verifications for permanent magnet biased magnetic bearings. Similarly Maslen et al. [9] showed analytical and experimental results on the design and construction of permanent magnet biased magnetic bearings. Lee et al. [10,11] provides extensive discussion of design, testing and performance limits of the permanent magnet biased magnetic bearings. Fan et al. [12] also suggested systematic design procedures for permanent magnet biased magnetic bearings.

The present work describes the theory and following numerical analysis for the novel fault-tolerant homopolar magnetic bearing. Energy efficient homopolar magnetic bearings with fault tolerant capability may find great use in some applications such as flywheel energy storage systems and momentum wheels.

2. Bearing model

The schematic drawing of an 8-active pole, permanent magnet biased homopolar magnetic bearing is shown in Fig. 1. Assuming that eddy current effects and material path reluctances are neglected, Maxwell's equations are reduced to the equivalent magnetic circuit for the homopolar magnetic bearing as shown in Fig. 2. The reluctance in air gap j of the active pole plane is

$$R_j = \frac{g_j}{\mu_0 a_0}, \tag{1}$$

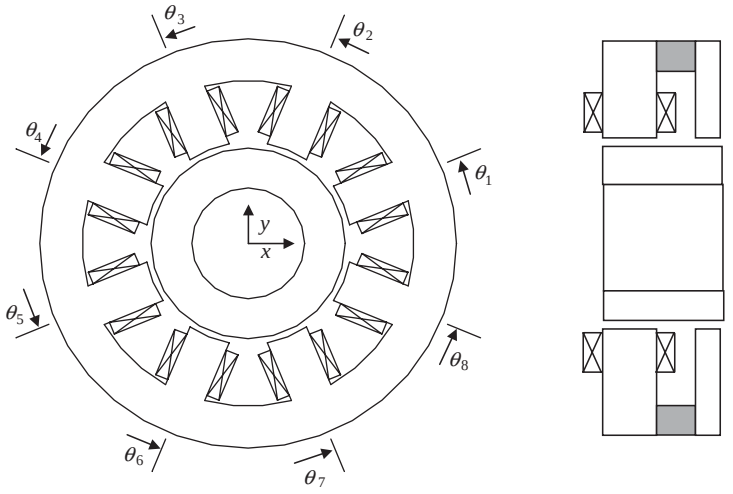

Fig. 1. Schematic of an 8-active pole, permanent magnet biased magnetic bearing.

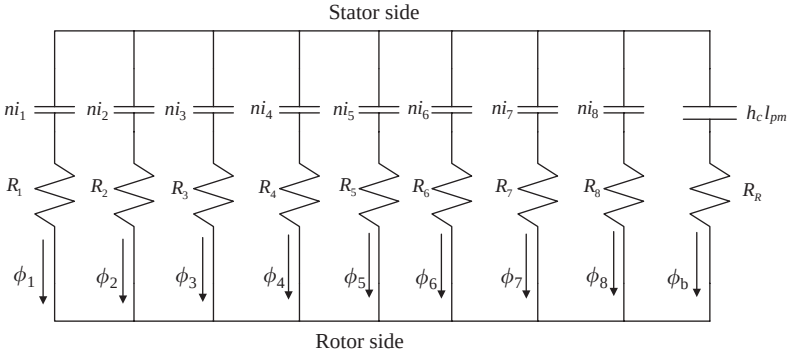

Fig. 2. Equivalent magnetic circuit.

where

$$g_j = g_0 - x\cos\theta_j - y\sin\theta_j. \tag{2}$$

Applying Ampere's law and Gauss's law to the magnetic circuit leads to a matrix equation,

$$\begin{bmatrix} R_1 & -R_2 & 0 & \cdot & \cdot & \cdot & 0 \\ 0 & R_2 & -R_3 & 0 & \cdot & \cdot & 0 \\ 0 & \cdot & \cdot & \cdot & \cdot & \cdot & \cdot \\ \cdot & \cdot & \cdot & \cdot & \cdot & \cdot & \cdot \\ \cdot & \cdot & \cdot & \cdot & \cdot & \cdot & 0 \\ 0 & \cdot & \cdot & \cdot & 0 & R_7 & -R_8 \\ 1 & 1 & \cdot & \cdot & \cdot & 1 & 1+\dfrac{R_8}{R_R} \end{bmatrix} \begin{bmatrix} \phi_1 \\ \phi_2 \\ \cdot \\ \cdot \\ \cdot \\ \cdot \\ \phi_7 \\ \phi_8 \end{bmatrix} = \begin{bmatrix} 0 \\ 0 \\ \cdot \\ \cdot \\ \cdot \\ 0 \\ \dfrac{h_c l_{pm}}{R_R} \end{bmatrix} + \begin{bmatrix} n & -n & 0 & \cdot & \cdot & \cdot & 0 \\ 0 & n & -n & 0 & \cdot & \cdot & 0 \\ 0 & \cdot & \cdot & \cdot & \cdot & \cdot & \cdot \\ \cdot & \cdot & \cdot & \cdot & \cdot & \cdot & \cdot \\ \cdot & \cdot & \cdot & \cdot & \cdot & \cdot & 0 \\ 0 & \cdot & \cdot & \cdot & 0 & n & -n \\ 0 & 0 & \cdot & \cdot & \cdot & 0 & \dfrac{n}{R_R} \end{bmatrix} \begin{bmatrix} i_1 \\ i_2 \\ \cdot \\ \cdot \\ \cdot \\ \cdot \\ i_7 \\ i_8 \end{bmatrix}, \tag{3}$$

or

$$R\Phi = H + NI. \tag{4}$$

The 8-pole homopolar magnetic bearing utilizes 8 number of coils each driven by its independent power amplifiers. The control currents distributed to the bearing are generally expressed as an 8×2 matrix T and control voltage vector v_c. The current vector is

$$I = Tv_c, \tag{5}$$

where

$$T = [T_x T_y], \quad v_c = \begin{bmatrix} v_{cx} \\ v_{cy} \end{bmatrix}.$$

For example a distribution matrix for an 8-pole homopolar bearing with independent currents is

$$\tilde{T} = \begin{bmatrix} \cos\frac{\pi}{8} & \sin\frac{\pi}{8} \\ \cos\frac{3\pi}{8} & \sin\frac{3\pi}{8} \\ \cos\frac{5\pi}{8} & \sin\frac{5\pi}{8} \\ \cos\frac{7\pi}{8} & \sin\frac{7\pi}{8} \\ \cos\frac{9\pi}{8} & \sin\frac{9\pi}{8} \\ \cos\frac{11\pi}{8} & \sin\frac{11\pi}{8} \\ \cos\frac{13\pi}{8} & \sin\frac{13\pi}{8} \\ \cos\frac{15\pi}{8} & \sin\frac{15\pi}{8} \end{bmatrix}.$$

The feedback control voltages v_{cx} and v_{cy}, determined with any type of control law and measured rotor motions, are distributed to each pole via $\tilde{T}$ in normal operation, and create effective stiffness and damping of the bearing to suspend the rotor around the bearing center position. With the uniform current distribution with $\tilde{T}$ as well as the symmetric bearing geometries, magnetic forces are (x, y) decoupled and vary linearly with respect to control currents and rotor displacements around the bearing center position. If symmetry is lost due to a coil failure, magnetic forces are no longer decoupled and linear with respect to control currents and rotor displacements, and even it may be difficult to maintain stable control. Reassigning the remaining currents with a redefined current distribution scheme may remedy this by providing the same decoupled magnetic forces as those before failure.

If some coils fail, the full (8×1) current vector is related to the reduced current vector by introducing a failure map matrix W.

$$I = W\hat{I}. \tag{6}$$

For example the matrix W for the 5–7–8th coils failed bearing is described as

$$W = \begin{bmatrix} 1 & 0 & 0 & 0 & 0 \\ 0 & 1 & 0 & 0 & 0 \\ 0 & 0 & 1 & 0 & 0 \\ 0 & 0 & 0 & 1 & 0 \\ 0 & 0 & 0 & 0 & 0 \\ 0 & 0 & 0 & 0 & 1 \\ 0 & 0 & 0 & 0 & 0 \\ 0 & 0 & 0 & 0 & 0 \end{bmatrix}.$$

The reduced distribution matrix $\hat{T}$ is defined as

$$\hat{I} = \hat{T} v_c, \tag{7}$$

where

$$\hat{T} = [\hat{T}_x \hat{T}_y], \tag{8}$$

$$\hat{T}_x = [t_1, t_2, \ldots, t_q]^{\mathrm{T}}, \quad \hat{T}_y = [t_{q+1}, t_{q+2}, \ldots, t_{2q}]^{\mathrm{T}}.$$

The parameter q represents the number of unfailed poles.

The flux densities in the active pole working air gaps are reduced with flux leakage, fringing, and saturation of magnetic material. The flux density vector in the air gaps with failed coils is described as

$$B = \varsigma A^{-1} R^{-1} (H + NW\hat{T} v_c), \tag{9}$$

where the pole face area matrix is $A = \mathrm{diag}([a_0, a_0, a_0, a_0, a_0, a_0, a_0, a_0])$. The flux density vector is then

$$B = Gv, \tag{10}$$

where

$$G = [\, G_b H \quad G_c \hat{T}_x \quad G_c \hat{T}_y \,], \quad v = \begin{bmatrix} 1 \\ v_x \\ v_y \end{bmatrix}, \tag{11}$$

$$G_b = \varsigma A^{-1} R^{-1}, \quad G_c = \varsigma A^{-1} R^{-1} NW.$$

Magnetic forces developed in the active pole plane are described as

$$f_x = v^{\mathrm{T}} M_x v, \tag{12}$$

$$f_y = v^{\mathrm{T}} M_y v, \tag{13}$$

where

$$M_x(\hat{T}) = -G^{\mathrm{T}} \frac{\partial D}{\partial x} G, \quad M_y(\hat{T}) = -G^{\mathrm{T}} \frac{\partial D}{\partial y} G, \tag{14}$$

and where the air gap energy matrix is;

$$D = \mathrm{diag}([g_j a_0/(2\mu_0)]). \tag{15}$$

3. Bias linearization

The magnetic forces in Eqs. (12) and (13) can be linearized about the bearing center position and the zero control voltages by using Taylor series expansion. The linearized magnetic forces are;

$$\begin{bmatrix} F_x \\ F_y \end{bmatrix} = -\begin{bmatrix} k_{pxx} & k_{pxy} \\ k_{pyx} & k_{pyy} \end{bmatrix} \begin{bmatrix} x \\ y \end{bmatrix} + \begin{bmatrix} k_{vxx} & k_{vxy} \\ k_{vyx} & k_{vyy} \end{bmatrix} \begin{bmatrix} v_{cx} \\ v_{cy} \end{bmatrix}. \tag{16}$$

The position stiffnesses are defined as

$$k_{p\varphi\omega} = -H^{\mathrm{T}} \frac{\partial Q_{\varphi b}}{\partial \omega}\bigg|_{\varphi=0\omega=0} H, \tag{17}$$

where

$$Q_{\varphi b} = -G_b \frac{\partial D}{\partial \varphi} G_b.$$

The parameters φ and ω represent either x or y. The position stiffnesses of the homopolar bearing remain unchanged with a coil failure since the position stiffnesses are only influenced by the bias flux driven with permanent magnets. The voltage stiffnesses are defined as

$$k_{v\varphi\omega} = 2H^{\mathrm{T}} Q_{b\varphi}\big|_{\varphi=0\omega=0} \hat{T}_{\omega}, \tag{18}$$

where

$$Q_{b\varphi} = -G_b \frac{\partial D}{\partial \varphi} G_c.$$

For example the direct voltage stiffness of an unfailed bearing with the distribution matrix of $\tilde{T}$ is

$$k_v = k_{v\varphi\varphi} = 2H^{\mathrm{T}} Q_{b\varphi}\big|_{\varphi=0\omega=0} \tilde{T}_{\varphi}. \tag{19}$$

Employing an optimal current distribution matrix T may decouple the linearized forces of the failed bearing, and even maintain the same decoupled magnetic forces as those of an unfailed magnetic bearing. Maslen and Meeker [1] introduced a linearization method which effectively decouple the control forces for a failed bearing by choosing a proper distribution matrix. Though not identified in [1], the direct voltage stiffness k_v is used to yield the same linearized control forces as those of the unfailed bearing. The necessary conditions to yield the same decoupled magnetic control forces are

$$M_x = k_v \begin{bmatrix} 0 & 1/2 & 0 \\ 1/2 & 0 & 0 \\ 0 & 0 & 0 \end{bmatrix}, \quad M_y = k_v \begin{bmatrix} 0 & 0 & 1/2 \\ 0 & 0 & 0 \\ 1/2 & 0 & 0 \end{bmatrix}. \tag{20}$$

If the distribution matrix $\hat{T}$ is determined such that Eq. (20) should be met, the magnetic forces at bearing center position in Eqs. (12) and (13) lead to

$$f_x = k_v v_{cx}, \quad f_y = k_v v_{cy}. \tag{21}$$

Eqs. (14) and (20) can be written in 18 scalar forms, and then boils down to 10 algebraic equations if redundant terms are eliminated. The equality constraints to yield the same control forces before and after failure are

$$\begin{aligned}
h_1(\hat{T}) &= \hat{T}_x^{\mathrm{T}} Q_{x0} \hat{T}_x = 0,\\
h_2(\hat{T}) &= \hat{T}_y^{\mathrm{T}} Q_{x0} \hat{T}_y = 0,\\
h_3(\hat{T}) &= H^{\mathrm{T}} Q_{bx0} \hat{T}_y = 0,\\
h_4(\hat{T}) &= \hat{T}_x^{\mathrm{T}} Q_{x0} \hat{T}_y = 0,\\
h_5(\hat{T}) &= H^{\mathrm{T}} Q_{bx0} \hat{T}_y = k_v/2,\\
h_6(\hat{T}) &= \hat{T}_x^{\mathrm{T}} Q_{y0} \hat{T}_x = 0,\\
h_7(\hat{T}) &= \hat{T}_y^{\mathrm{T}} Q_{y0} \hat{T}_y = 0,\\
h_8(\hat{T}) &= H^{\mathrm{T}} Q_{by0} \hat{T}_x = 0,\\
h_9(\hat{T}) &= \hat{T}_x^{\mathrm{T}} Q_{y0} \hat{T}_y = 0,\\
h_{10}(\hat{T}) &= H^{\mathrm{T}} Q_{by0} \hat{T}_y = k_v/2,
\end{aligned} \tag{22}$$

where

$$Q_{\varphi b0} = -G_b \frac{\partial D}{\partial \varphi} G_b \bigg|_{\varphi=0\omega=0}, \quad Q_{b\varphi 0} = -G_b \frac{\partial D}{\partial \varphi} G_c \bigg|_{\varphi=0\omega=0}, \quad Q_{\varphi 0} = -G_c \frac{\partial D}{\partial \varphi} G_c \bigg|_{\varphi=0\omega=0}.$$

4. Optimal distribution matrix solutions

There may exist multiple candidates of $\hat{T}$'s that satisfy the necessary conditions described in Eq. (22). The criterion for choosing the best candidate is the one that will yield the maximum load capacity prior to any saturation. To accomplish this a distribution matrix $\hat{T}$ can be determined by using the Lagrange Multiplier method to minimize the Euclidean norm of the flux density vector B [3]. The cost function is defined as

$$J = B(\hat{T})^{\mathrm{T}} P B(\hat{T}), \tag{23}$$

where the diagonal weighting matrix P is also selected to maximize the load capacity.

The Lagrange Multiplier method is then used to solve for $\hat{T}$ that satisfies Eq. (22). Define:

$$L(\hat{T}) = B(\hat{T})^{\mathrm{T}} P B(\hat{T}) + \sum_{j=1}^{10} \lambda_j h_j(\hat{T}). \tag{24}$$

Partial differentiation of Eq. (24) with respect to t_i and λ_j leads to $2q+10$ non-linear algebraic equations to solve for t_i and λ_j.

$$\Psi = \begin{bmatrix} \psi_1(t,\lambda) \\ \psi_2(t,\lambda) \\ \cdot \\ \cdot \\ \cdot \\ \psi_{2q+9}(t,\lambda) \\ \psi_{2q+10}(t,\lambda) \end{bmatrix} = 0, \tag{25}$$

where

$$\psi_i = \frac{\partial L}{\partial t_i} = 0, \quad i = 1,2,\ldots,2q, \tag{26}$$

$$\psi_{2q+j} = h_j(\hat{T}) = \quad 0, \quad j = 1,2,\ldots,10. \tag{27}$$

Eq. (25) can be solved for t_i and λ_j numerically by any non-linear algebraic equation solver. Since the cost function is not convex and equality constraints are not affine, there may exist multiple local optima. Various initial guesses of t_i and λ_j can be tested to find a better solution of $\hat{T}$.

Some examples of distribution matrices are calculated for the 8-pole homopolar magnetic bearing with the nominal air gap g_0 (0.508 mm), pole face area a_0 (602 mm^2), number of coil turns n(50 turns). It is assumed that permanent magnets are selected to produce bias flux density of 0.6 T in the air gaps of the active pole plane. The design of the permanent magnets for a homopolar magnetic bearing is beyond the scope of this paper. The direct voltage stiffness k_v is then calculated as 106.651 N/V. A distribution matrix for an 8-pole homopolar bearing with the 7–8th coils failed operation is calculated as

$$T_{78} = \begin{bmatrix} 1.9337 & -0.5171 \\ -0.7557 & 2.1604 \\ -0.2844 & 0.3313 \\ -0.3109 & 0.2836 \\ -2.1707 & 0.7506 \\ 0.5313 & -1.9159 \\ 0 & 0 \\ 0 & 0 \end{bmatrix}. \tag{28}$$

Eq. (14) is satisfied with the calculated T_{78} as shown in

$$M_x = \begin{bmatrix} 0 & 53.3254 & -0.0005 \\ 53.3254 & -0.0084 & -0.0097 \\ -0.0005 & -0.0097 & -0.0196 \end{bmatrix}, \quad M_y = \begin{bmatrix} 0 & 0 & 53.3247 \\ 0 & 0.0148 & 0.0106 \\ 53.3247 & 0.0106 & 0.0092 \end{bmatrix}.$$

A distribution matrix with the 6–7–8th coils failed operation is calculated as

$$T_{678} = \begin{bmatrix} 1.5852 & 0.5941 \\ -0.9194 & 1.4034 \\ -0.5185 & 1.2468 \\ -0.3469 & 1.6607 \\ -2.2336 & -0.0018 \\ 0 & 0 \\ 0 & 0 \\ 0 & 0 \end{bmatrix}, \tag{29}$$

$$M_x = \begin{bmatrix} 0 & 53.3195 & 0.0019 \\ 53.3195 & -0.2224 & 0.2098 \\ 0.0019 & 0.2098 & -0.0971 \end{bmatrix}, \quad M_y = \begin{bmatrix} 0 & 0.0023 & 53.3134 \\ 0.0023 & 0.3003 & -0.0071 \\ 53.3134 & -0.0071 & 0.5396 \end{bmatrix}.$$

A distribution matrix with the 5–6–7–8th coils failed operation is calculated as

$$T_{5678} = \begin{bmatrix} 1.8351 & 0.8207 \\ 0.2480 & 1.6421 \\ -0.2480 & 1.6422 \\ -1.8351 & 0.8206 \\ 0 & 0 \\ 0 & 0 \\ 0 & 0 \\ 0 & 0 \end{bmatrix}, \tag{30}$$

$$M_x = \begin{bmatrix} 0 & 51.6665 & -0.0005 \\ 51.6665 & 0.0002 & 2.4646 \\ 0 & 2.4646 & -0.0005 \end{bmatrix}, \quad M_y = \begin{bmatrix} 0 & 0 & 52.8487 \\ 0 & 6.3107 & 0 \\ 52.8487 & 0 & 3.0923 \end{bmatrix}.$$

A distribution matrix with the 4–5–6–7th–8th coils failed operation is calculated as

$$T_{45678} = \begin{bmatrix} 2.3563 & 0.2173 \\ 0.7656 & 1.8217 \\ -1.5431 & 1.8800 \\ 0 & 0 \\ 0 & 0 \\ 0 & 0 \\ 0 & 0 \\ 0 & 0 \end{bmatrix}, \tag{31}$$

Table 1
The calculated voltage stiffnesses for the failed bearing

Voltage stiffness (N/V)	$\tilde{T}$	T_{78}	T_{678}	T_{5678}	T_{45678}
k_{vxx}	106.651	106.650	106.639	103.333	88.3227
k_{vxy}	0	−0.001	0.0037	0	5.1514
k_{vyx}	0	0	0.0047	0	5.2926
k_{vyy}	106.651	106.649	106.627	105.697	101.096

$$M_x = \begin{bmatrix} 0 & 44.1613 & 2.5757 \\ 44.1613 & 7.7930 & 1.6296 \\ 2.5757 & 1.6296 & -0.4714 \end{bmatrix}, \quad M_y = \begin{bmatrix} 0 & 2.6463 & 50.5479 \\ 2.6463 & 11.2544 & -4.5018 \\ 50.5479 & -4.5018 & 7.4300 \end{bmatrix}.$$

Similarly, the distribution matrices can be calculated for a failed homopolar bearing up to all combinations of 5 coils failed out of 8 coils. In the previous fault tolerant scheme with heteropolar magnetic bearings [3,4], distribution matrix solutions do not exist for a certain combination of 5 failed coils (for example, no solution exists for 5 adjacent coils failed heteropolar bearings). No solutions exist if more than 5 coils fail for the homopolar magnetic bearing since at least 3 independent currents are required to generate arbitrary forces in a magnetic bearing [13].

The calculated voltage stiffnesses of the bearing with the distribution matrices of Eqs. (28)–(31) are shown in Table 1. Table 1 shows that the linearized magnetic forces of the homopolar magnetic bearing actuator remain very much unchanged even though any of the distribution matrices of $\tilde{T}$, T_{78}, T_{678}, T_{5678}, and T_{45678} are used in case of failure. However, the overall load capacity of the bearing is reduced as coils fail. The same magnetic forces are then preserved up to the load capacity of the failed bearing. The load capacities of the multiple poles failed homopolar magnetic bearing are calculated for the distribution matrices of T_{78}, T_{678}, T_{5678}, and T_{45678} and shown in Fig. 3. The outer locus shows the maximum load capacity of the unfailed bearing, whereas the inner locus shows the failed bearing load capacities for eight directions. It is notable that the load capacities before magnetic saturation for the failed homopolar magnetic bearing are greatly improved compared to those of heteropolar magnetic bearings shown in Ref. [3]. The maximum load capacity of the unfailed homopolar magnetic bearing is calculated to be 680 N. The load capacity of 5 straight coils failed bearing is reduced to 230 N (34% of the full load capacity).

5. Control system design and simulations

The schematic of a fault-tolerant control scheme utilizing distribution matrices developed in the previous section is shown in Fig. 4. The controller consists of two independent parts, which are a feedback voltage control law and an adaptive current distribution mechanism. Though any control algorithm for magnetic bearing systems appearing in the literature can be utilized with the

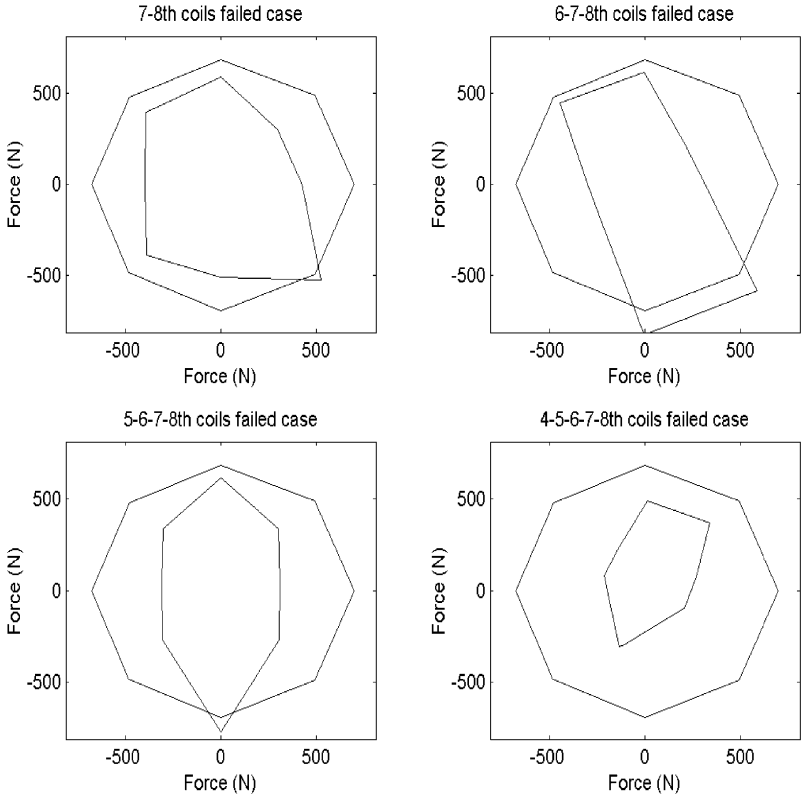

Fig. 3. Load capacities of the failed homopolar magnetic bearings.

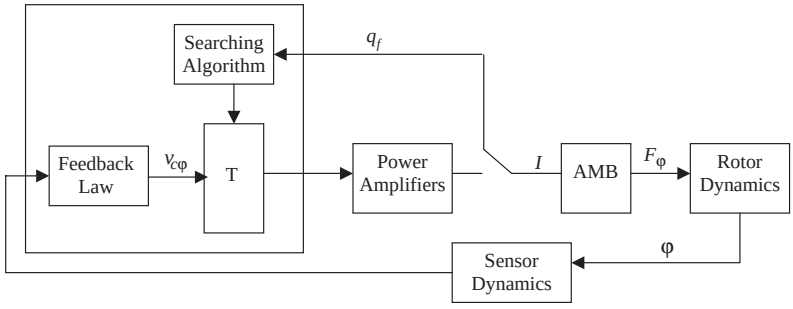

Fig. 4. Schematic of the fault-tolerant controller.

fault tolerant scheme, for sake of illustration, a simple PD feedback control law is used to stabilize the system.

$$v_{c\varphi} = K_p\varphi + K_d\dot{\varphi}, \tag{32}$$

$$\varphi \in (x, y).$$

While the feedback control law remains unaltered during the failure the appropriate current distribution matrix T can be continuously updated using an adaptive current distribution mechanism. The fault-tolerant control scheme can be easily implemented in a physical controller (DSP). By prior experience [4] this series of actions for failure detection, searching for T, and replacement by the new T can be implemented in one loop time of a fast (>15 K/s) DSP controller.

The fault-tolerant control system is simulated on a horizontal flexible rotor supported on the homopolar bearings. A finite element model of the flexible rotor with 38 elements is shown in Fig. 5. The flexible rotor has mass of 10.7 kg, length of 0.7 m. Two radial magnetic bearings are located at 0.1235 m from the ends. The flexible rotor is discretized into a reasonable number of elements which consist of a series of massless beam elements and lumped mass and inertias. The mass, polar moment of inertia, and transverse moment of inertia are halved and placed at each node. The equation of motion for the flexible rotor is then described as

$$M\ddot{X} + G\dot{X} + KX = F, \tag{33}$$

where M, G, and K represent mass, gyroscopic moment, and stiffness matrices, respectively. External forces exerted on the system of equations are described as

$$F = F_m + F_g + F_u, \tag{34}$$

F_m, F_g, and F_u represent magnetic force, gravity force, and unbalanced force vectors, respectively. The magnetic force vector is

$$F_m = \tilde{H}\tilde{F}, \tag{35}$$

where

$$\tilde{F} = \begin{bmatrix} f_x^A & f_y^A & f_x^B & f_y^B \end{bmatrix}^{\mathrm{T}},$$

and where $\tilde{H}$ assigns magnetic forces to the corresponding states.

The following system dynamics simulation illustrates the transient response of a rotor supported by magnetic bearings during a coil failure event. An unbalance force of $me\Omega^2$ with m(2.0 g), e(0.01 m) and Ω(spinning speed) are applied at the two bearing locations. The distribution matrix of $\tilde{T}$ is switched to T_{5678} and T_{45678} when 4 adjacent coils failed at 0.02 s and then 5 adjacent coils failed at 0.04 s. The rotor speed is held constant at 20,000 r.p.m. Fig. 6 shows transient response of the current inputs to the outboard bearing from the normal unfailed operation through the 5–6–7–8th coils and 4–5–6–7–8th coils of the outboard bearing failed at 0.02 s and 0.04 s, respectively. Fig. 7 shows the corresponding transient response of the flux densities in the outboard bearing for the 5–6–7–8th coils and 4–5–6–7–8th coils failed operation.

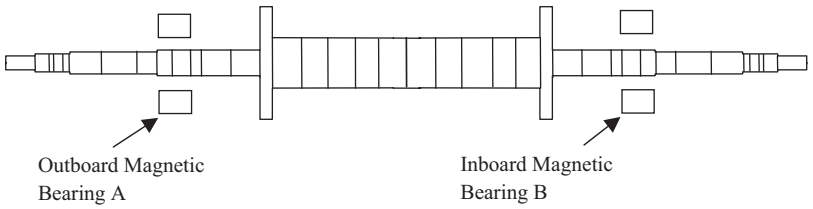

Fig. 5. Finite element model of the flexible rotor.

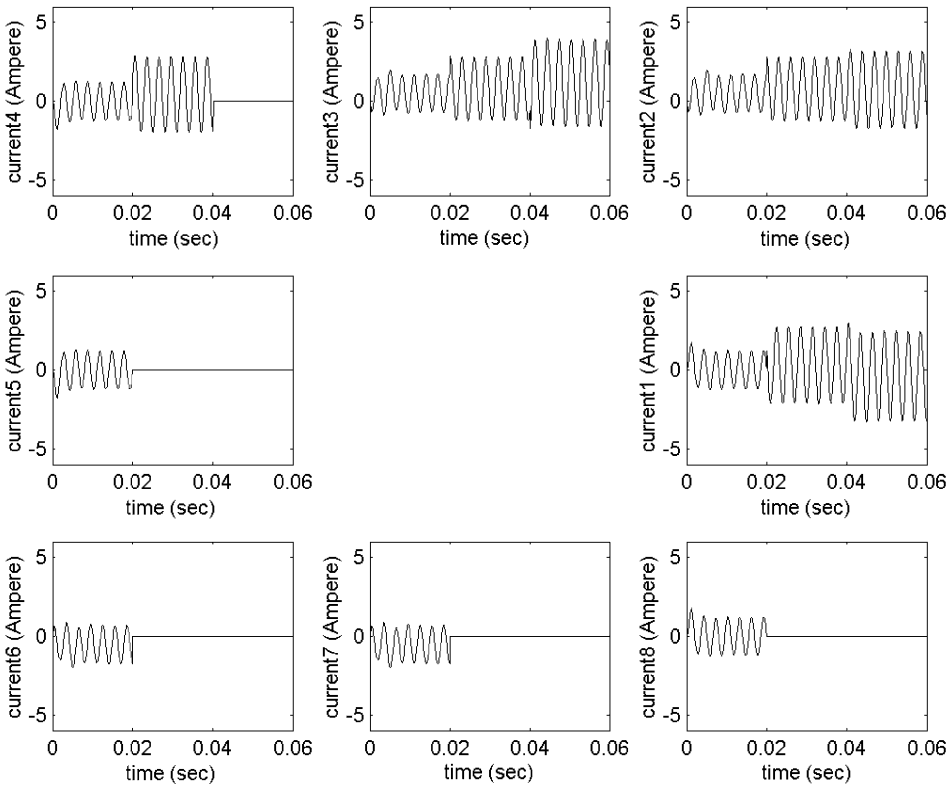

Fig. 6. Current plot for a series of failures.

Figs. 8 and 9 show transient rotor displacements and transient orbits at the outboard bearing for the 5–6–7–8th coils and 4–5–6–7–8th coils failed operation respectively. Figs. 6–9 indicates that very much the same rotordynamic responses are maintained throughout the series of failure events, while currents and fluxes in the homopolar magnetic bearing change significantly.

6. Conclusions

A fault tolerant control scheme is developed for an energy efficient homopolar magnetic bearing. The homopolar bearing actuator using the fault tolerant control algorithm can preserve the same linearized magnetic forces by redistributing the remaining currents even if some components such as coils or power amplifiers suddenly fail. The distribution matrix T of control voltages is determined by using the Lagrange Multiplier optimization with equality constraints for a failed bearing in a manner that the load capacity should be maximized. Simulations show that very much the same vibrations (orbits or displacements) are maintained throughout failure events while currents and fluxes change significantly with different distribution scheme.

Only control currents as well as control fluxes are redistributed for the failed bearing while bias flux driven by permanent magnets remains constant. Less strict constraints of only 10 equations are required for the fault tolerant homopolar bearing to produce the same magnetic forces, while

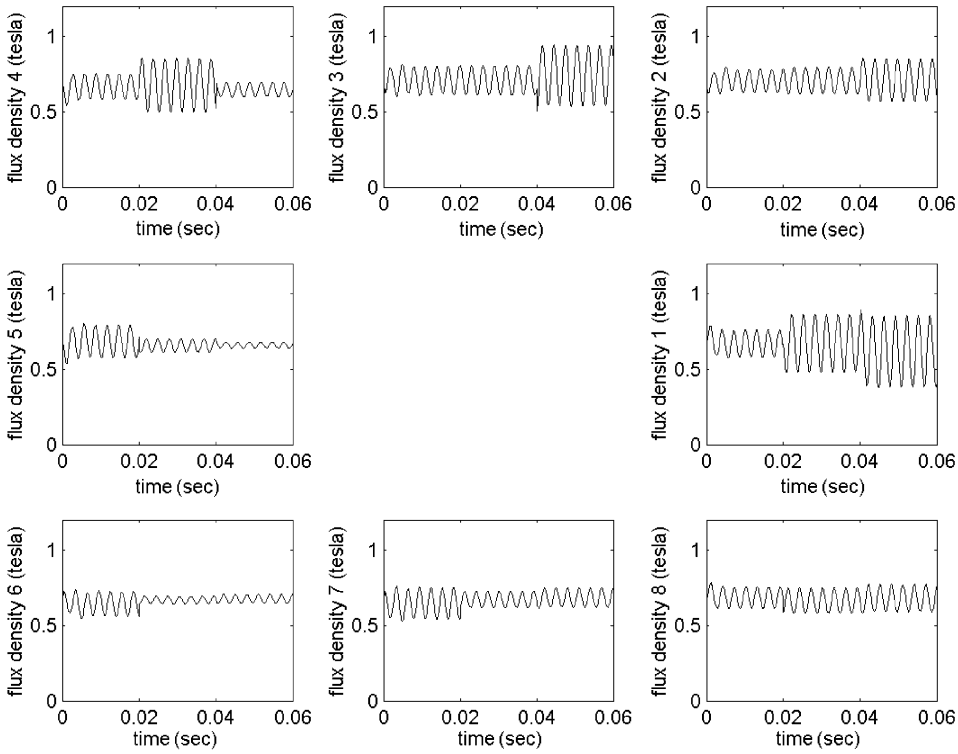

Fig. 7. Flux density plot for a series of failures.

12 constraint equations are required for the fault tolerant heteropolar bearing in Ref. [3]. This released conditions may give some benefits to the realization of fault tolerant homopolar bearings. The solution space of distribution matrices is extended for the homopolar bearing. The distribution matrices can be calculated for a failed homopolar bearing up to all combinations of 5 coils failed out of 8 coils. In the previous fault tolerant scheme with heteropolar magnetic bearings, no solutions exist for certain combinations of 5 failed coils. The load capacities of the failed homopolar magnetic bearings are greatly increased compared to those of heteropolar magnetic bearings.

Fault tolerance of the magnetic bearing actuator is achieved at the expense of additional hardware requirements and reduction of overall bearing load capacity. Therefore, the fault tolerant magnetic bearing should be designed enough to support loads even in case of a severe failure (5 coils failed out of 8 coils). Otherwise, disturbances from unbalance, runouts, and sideloads should be maintained at low level to prevent saturation.

Appendix A. Nomenclature

a_0 pole face area of an active pole
A diagonal matrix of pole face area a_0
g_0 nominal air gap in active pole plane

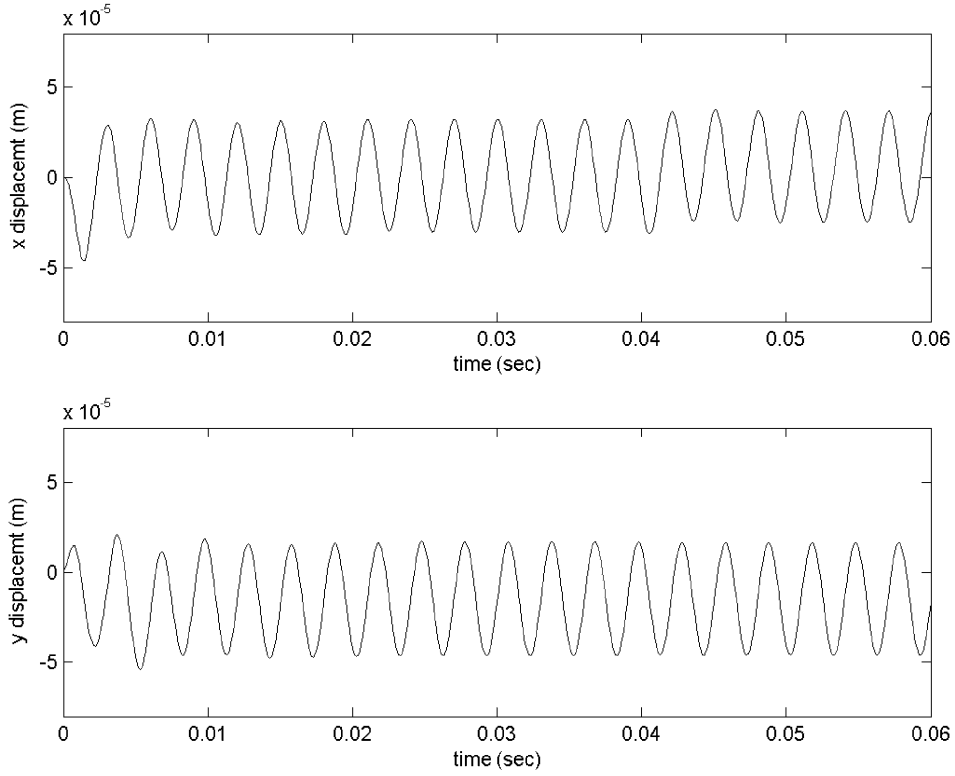

Fig. 8. Displacement plot for a series of failures.

h_c coercive force of a permanent magnet
i_j currents through the jth pole
I current vector
K_p, K_d proportional and derivative gains
l_{pm} length of a permanent magnet
n number of coil turns
q Number of unfailed poles
R_j air gap reluctance of the jth pole
R_R return path reluctance
x, y journal displacements
μ_0 permeability of air
ς flux fringing factor
ϕ_j flux through the jth pole
v_{cx}, v_{cy} x and y control voltages
Ω rotating speed
θ_j pole angle of the jth pole
T current distribution matrix

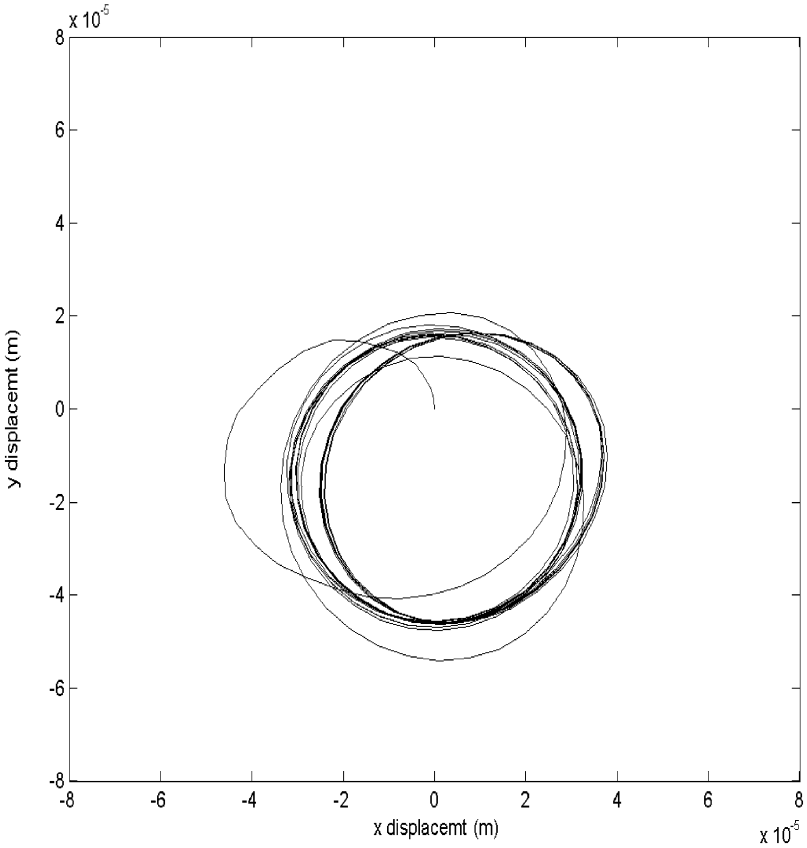

Fig. 9. Orbit plot for a series of failures.

References

[1] E.H. Maslen, D.C. Meeker, Fault tolerance of magnetic bearings by generalized bias current linearization, *IEEE Transactions on Magnetics* 31 (1995) 2304–2314.

[2] E.H. Maslen, C.K. Sortore, G.T. Gillies, R.D. Williams, S.J. Fedigan, R.J. Aimone, A fault tolerant magnetic bearings, *American Society of Mechanical Engineers Journal of Engineering for Gas Turbines and Power* 121 (1999) 504–508.

[3] U.J. Na, A.B. Palazzolo, Optimized realization of fault-tolerant heteropolar magnetic bearings for active vibration control, *American Society of Mechanical Engineers Journal of Vibration and Acoustics* 122 (2000) 209–221.

[4] U.J. Na, A.B. Palazzolo, A. Provenza, Test and theory correlation study for a flexible rotor on fault-tolerant magnetic bearings, *American Society of Mechanical Engineers Journal of Vibration and Acoustics* 124 (2002) 359–366.

[5] U.J. Na, A.B. Palazzolo, The fault-tolerant control of magnetic bearings with reduced controller outputs, *American Society of Mechanical Engineers Journal of Dynamic Systems Measurement and Control* 123 (2001) 219–224.

[6] M.E.F. Kasarda, P.E. Allaire, P.M. Norris, C. Mastrangelo, E.H. Maslen, Experimentally determined rotor power losses in homopolar and heteropolar magnetic bearings, *American Society of Mechanical Engineers Journal of Engineering for Gas Turbines and Power* 121 (1999) 697–702.

[7] C.K. Sortore, P.E. Allaire, E.H. Maslen, R.R. Humphris, P.A. Studer, Permanent magnet biased magnetic bearings—design, construction and testing, *Proceedings of the Second International Symposium on Magnetic Bearings*, Tokyo, Japan, 1990, pp. 175–182.
[8] P.E. Allaire, E.H. Maslen, R.R. Humphris, C.K. Sortore, P.A. Studer, Low power magnetic bearing design for high speed rotating machinery, *Proceedings of the NASA International Symposium on Magnetic Suspension Technology*, 1992, pp. 317–329.
[9] E.H. Maslen, P.E. Allaire, M.D. Noh, C.K. Sortore, Magnetic bearing design for reduced power consumption, *American Society of Mechanical Engineers Journal of Tribology* 118 (1996) 839–846.
[10] A.C. Lee, F.Z. Hsiao, D. Ko, Analysis and testing of a magnetic bearing with permanent magnets for bias, *JSME International Journal Series C* 37 (1994) 774–782.
[11] A.C. Lee, F.Z. Hsiao, D. Ko, Performance limits of permanent-magnet-biased magnetic bearings, *JSME International Journal Series C* 37 (1994) 783–794.
[12] Y. Fan, A. Lee, F. Hsiao, Design of a permanent/electromagnetic magnetic bearing-controlled rotor system, *Journal of the Franklin Institute* 334B (1997) 337–356.
[13] D.C. Meeker, Optimal Solutions to the Inverse Problem in Quadratic Magnetic Actuators, Ph.D. Dissertation, School of Engineering and Applied Science, University of Virginia, Charlottesville, VA, 1996.